Neuron, volume *60*

Supplemental Data

V3 Spinal Neurons Establish a Robust and Balanced Locomotor Rhythm during Walking

Ying Zhang, Sujatha Narayan, Eric Geiman, Guillermo M. Lanuza, Tomoko Velasquez, Bayle Shanks, Turgay Akay, Jason Dyck, Keir Pearson, Simon Gosgnach, Chen-Ming Fan, and Martyn Goulding

Supplemental Figure 1

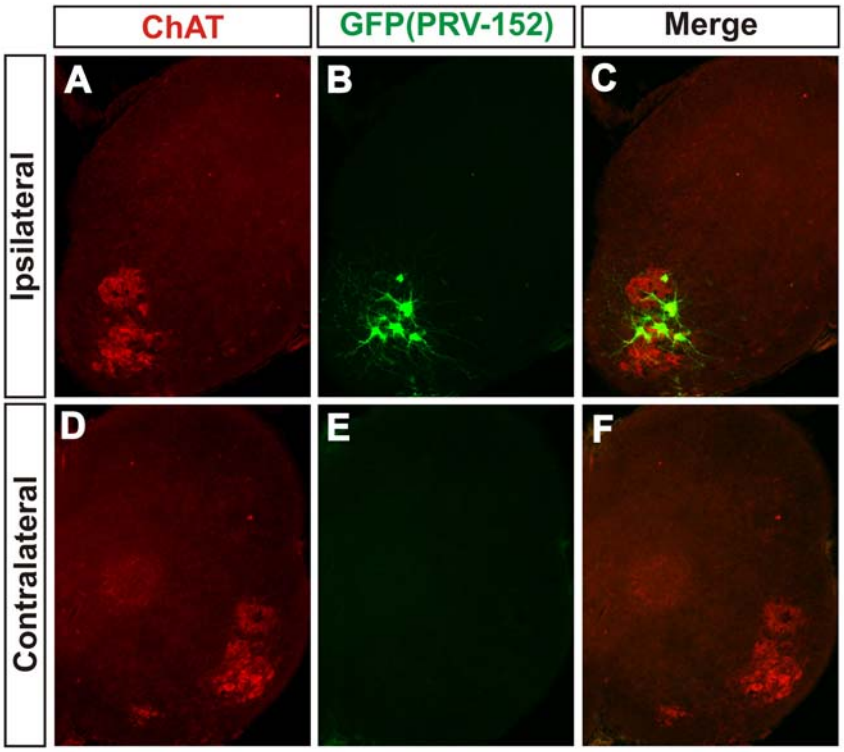

Figure S1. GFP-labeling of motor neurons 30h following PRV152 injection into the gastrocnemius muscle.

Injections of PRV152 into the gastrocnemius muscle (unilateral) of P1 neonate mice were made using the protocol described by Kerman et al. (2003) and Lanuza et al., (2004).

(A-F) Analysis of PRV infection in the lumbar spinal cord shows GFP-expression is restricted to ChAT-positive motor neurons that innervate the injected gastrocnemius muscle (A-C). No GFP-labeled neurons were seen observed on the contralateral side of the cord (D-F), nor did we observe interneurons ipsilateral to the injection site (A-C).

Supplemental Figure 2

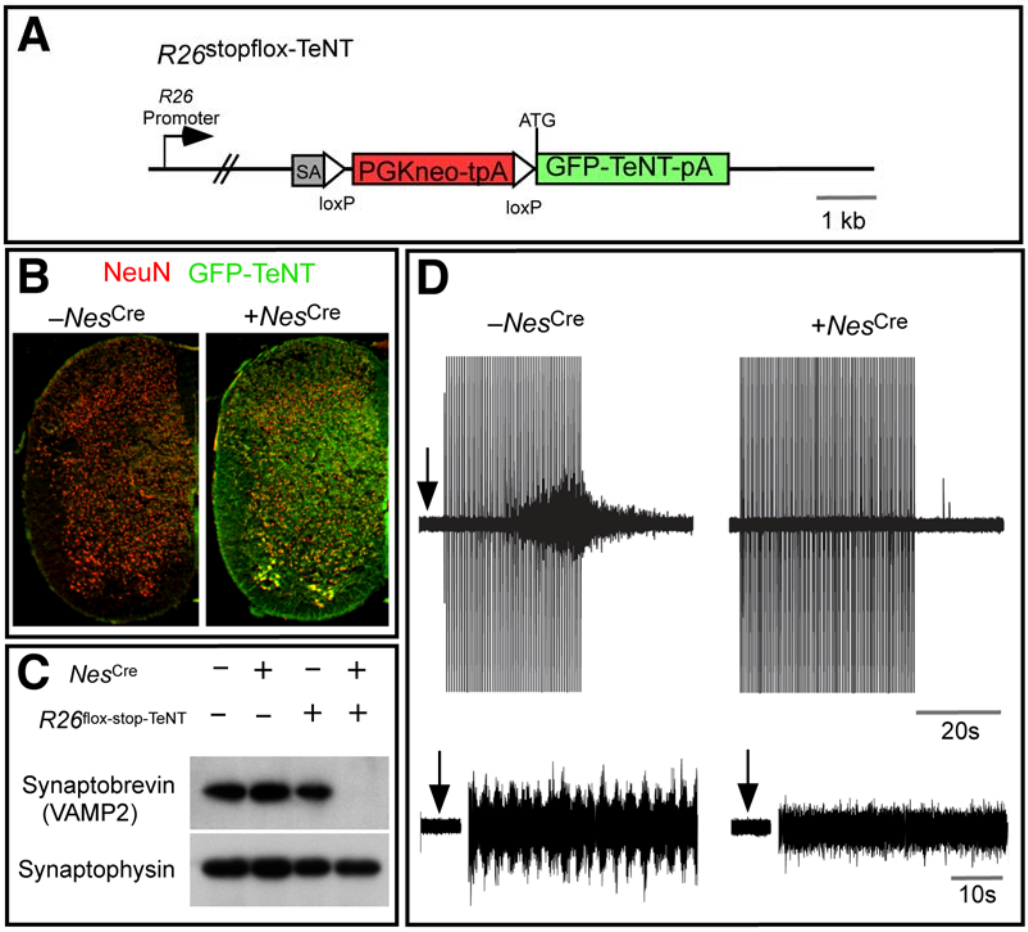

Figure S2. Efficient blockade of synaptic transmission in *R26*$^{\text{floxstop-TeNT}}$ mice.

(A) Schematic representation of the conditional *R26*$^{\text{floxstop- TeNT}}$ allele. This strain was created by targeting the *Rosa26* locus with a construct containing a splice acceptor (SA),

a loxp-flanked PGKNeo cassette (floxstop) followed by a GFP-TeNT fusion coding sequence.

(B) *Nestin*^{Cre} mice were crossed with *R26*$^{\text{floxstop-TeNT}}$ mice to induce a generalized expression of GFP-TeNT. Lumbar spinal cord sections from E18.5 mice were labeled with antibodies to the pan-neuronal marker NeuN (red) and GFP (green). In the spinal cord of *R26*$^{\text{floxstop-TeNT}}$ mice (Cre negative), no ectopic expression of GFP-TeNT was found.

(C) Western blot analysis shows a >100 fold decrease in the levels of VAMP2/synaptobrevin in protein extracts from *Nestin*^{Cre}*; R26*$^{\text{floxstop-TeNT}}$ E18.5 spinal cord.

(D) Upper: L2 ventral root activity evoked by the electric stimulation on contralateral dorsal root (2 Hz, cL5) of *R26*$^{\text{floxstop-TeNT}}$ (left) and Nestin$^{\text{Cre}}$; *R26*$^{\text{floxstop-TeNT}}$ (right) isolated E18.5 spinal cords. Bottom: Ventral root ENG recordings from an L2 ventral root before (arrow) and after the addition of NMDA/5-HT. While rhythmic activity is induced in *R26*$^{\text{floxstop-TeNT}}$ isolated cords (left), the addition of the agonists to *Nestin*^{Cre}*; R26*$^{\text{floxstop-TeNT}}$ spinal cord only produced tonic activity, indicating that motor neurons in the *Nestin*^{Cre}*; R26*$^{\text{floxstop-TeNT}}$ cords can be excited, however, synaptic transmission between spinal neurons that is necessary for fictive locomotion is largely blocked.

Supplemental Figure 3

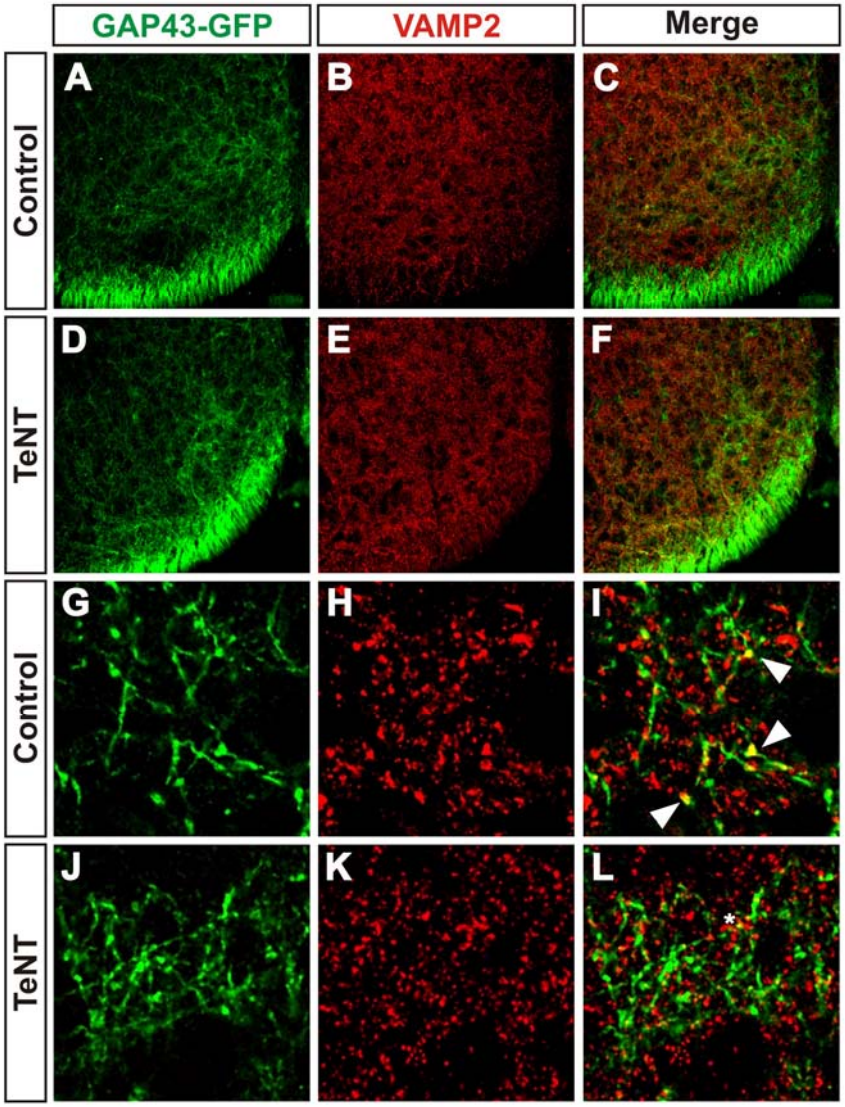

Figure S3. Selective reduction of VAMP2/synaptobrevin in V3-derived axons in the ventral horn of the *Sim1*^{Cre}; *R26*$^{flox\text{-}stop\text{-}TeNT}$ animals.

Sim1^{Cre}-dependent expression of the small tetanus toxin subunit (TeNT) in V3-derived neurons leads to the selective loss of VAMP2/synpatobrevin in the axonal processes of these cells. The *R26*$^{floxstop\text{-}GAP43\text{-}GFP}$ reporter was used to mark the axonal processes of V3-derived neurons.

(A-F) Cross sections through the ventral horn showing the overall level of VAMP2 expression (red) is largely unaltered in the cord of a *Sim1*^{Cre}; *R26*$^{floxstop\text{-}TeNT;}$ *R26*$^{floxstop\text{-}GAP43\text{-}GFP}$ animal (B) compared to a control *Sim1*^{Cre}; *R26*$^{floxstop\text{-}GAP43\text{-}GFP}$ cord (E).

(G-L) Large VAMP2 clusters are observed in GAP43-GFP^{+} V3 axons in the control cord (G-I, see arrowheads in I), but are absent from the axons of V3-derived neurons in the *Sim1*^{Cre}; *R26*$^{floxstop\text{-}TeNT}$; *R26*$^{floxstop\text{-}GAP43\text{-}GFP}$ cord. Some small VAMP2 punta were still observed in *Sim1*^{Cre}; *R26*$^{floxstop\text{-}TeNT}$; *R26*$^{floxstop\text{-}GAP43\text{-}GFP}$ sections, however, it is unclear whether these puncta represent V3 synaptic contacts.

Supplemental Figure 4

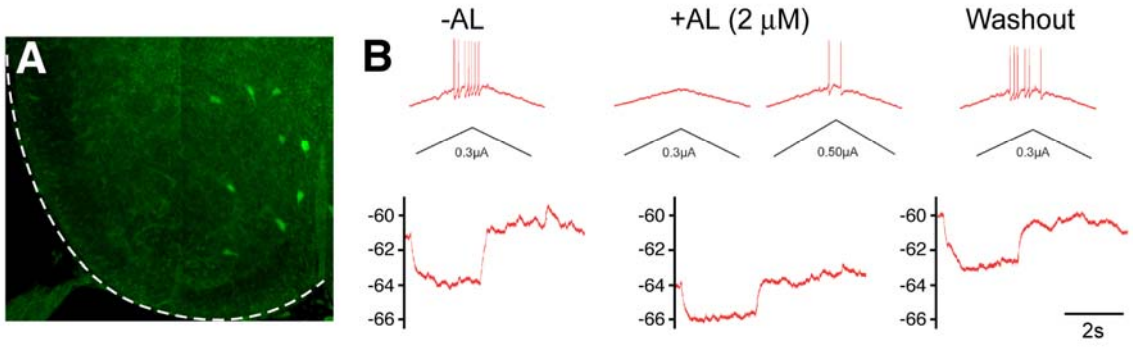

Figure S4. Allatostatin-dependent silencing of V3-derived neurons in the *Sim1*^{Cre}; *AlstR192* cord.

Changes in V3 neuron excitability in response to activating the allatostatin receptor were determined by performing whole cell recordings on GFP^{+} V3 neurons in slices taken from P1-P2 *Sim1*^{Cre}; AlstR192 cords (n=11 cells). Following application of allatostatin, V3-derived cells exhibited hyperpolarizing changes in membrane potential (range -0.4mV to -3.3mV, ave = 1.7±0.7mV) coupled with decreases in input resistance. Some

variability in the response of individual cells to allatostatin was noted. These differential effects on excitability may be due to different levels in GFP transgene expression in the V3 population (A).

(A) Section through a P1 *Sim1*^{Cre}; AlstR192 cord GFP expressing cells in the ventral horn. The *AlstR192* transgene contains an IRES-GFP cassette downstream of the allatostatin receptor gene (Gosgnach et al., 2006). GFP expression was visualized with an antibody to GFP. Note the variable expression of the AlstR-GFP transgene in V3-derived neurons.

(B) Recordings from a ventrally located V3 neuron in response to a current ramp. (Upper panels) Before application of allatostatin (AL) the cell fires multiple action potentials in response to a 0.3μA ramp, but fails to do so in the presence of allatostatin (100nM). This reversed upon washout of the allatostatin peptide (right). (Lower panels) Addition of allatostatin results in a decrease in the membrane potential of the cells coupled with a lowering of the membrane resistance.